

Radiation Damage to Alkyl Chain Monolayers on Semiconductor Substrates Investigated by Electron Spectroscopy

Fabrice Amy,^{†,‡} Calvin K. Chan,[†] Wei Zhao,[†] Jaehyung Hyung,[†] Masaki Ono,[§] Tomoki Sueyoshi,[§] Satoshi Kera,[§] Guy Neshet,^{||} Adi Salomon,^{||} Lior Segev,^{||} Oliver Seitz,^{||} Hagay Shpaisman,^{||} Achim Schöll,[⊥] Marc Haeming,[⊥] Till Böcking,[⊗] David Cahen,^{||} Leeor Kronik,^{||} Nobuo Ueno,[§] Eberhard Umbach,[⊥] and Antoine Kahn^{*,†}

Department of Electrical Engineering, Princeton University, Princeton, New Jersey 08544, Faculty of Engineering and Graduate School of Science & Technology, Chiba University, Chiba, Japan, Department of Materials and Interfaces, Weizmann Institute of Science, Rehovot, Israel, Experimental Physics II, University of Würzburg, Am Hubland, Würzburg, Germany, and School of Physics, University of New South Wales, Sydney, Australia

Received: June 9, 2006; In Final Form: August 26, 2006

Monolayers of alkyl chains, attached through direct Si–C bonds to Si(111), via phosphonates to GaAs(100) surfaces, or deposited as alkyl-silane monolayers on SiO₂, are investigated by ultraviolet and inverse photoemission spectroscopy and X-ray absorption spectroscopy. Exposure to ultraviolet radiation from a He discharge lamp, or to a beam of energetic electrons, leads to significant damage, presumably associated with radiation- or electron-induced H-abstraction leading to carbon–carbon double-bond formation in the alkyl monolayer. The damage results in an overall distortion of the valence spectrum, in the appearance of (occupied) states above the highest occupied molecular orbital of the alkyl molecule, and in a characteristic (unoccupied state) π^* resonance at the edge of the carbon absorption peak. These distortions present a serious challenge for the interpretation of the electronic structure of the monolayer system. We show that extrapolation to zero damage at short exposure times eliminates extrinsic features and allows a meaningful extraction of the density of state of the pristine monolayer from spectroscopy measurements.

Introduction

Self-assembled monolayers (SAMs) provide a wide range of possibilities for tailoring surface properties, such as reactivity, wetting, friction, optical, and electronic properties. SAMs have therefore become of central importance for research in many areas of physics, chemistry, biology, and engineering. Molecules consisting of a simple carbon chain backbone (alkanes) also constitute the basic element of a variety of plastic polymers such as polyethylene and fluoropolymers with a wide range of applications.

The structural simplicity of alkanes and their ability to form high-quality, dense monolayers make them ideal model systems for SAMs. Modified alkanes can be used to bind the chains chemically to a substrate, via S atoms to noble metals or semiconductors such as GaAs, via oxygen to various semiconductors and insulators (e.g., SiO₂), or directly, for example, via Si–C bonds to Si. Understanding the electronic structure of these prototypical systems is therefore of prime importance for determining and understanding the phenomena that dominate charge transport through isolated molecules or molecules arranged in monolayers, a primary goal of basic research in the field of molecular electronics.

Though chemically very stable, alkyl chains show some degradation under irradiation (X-ray, UV, and electron beam).^{1–5} Degradation mechanisms under irradiations have been identified as corresponding to the loss of F or H,⁶ bond scission, double-bond formation,⁵ cross-linking,^{6,7} and changes in chemistry at the substrate/chain interface.⁴ In the case of thin films, advantage can be taken of these degradations to further tailor the properties of the surface or interface. Indeed, applications such as photomicro machining⁷ or photodoping⁸ of thin films have been demonstrated. However, degradation also presents a serious challenge for investigation of the intrinsic electronic structure of alkyl SAMs with electron spectroscopy techniques, such as ultraviolet photoemission spectroscopy (UPS) for occupied states and inverse photoemission spectroscopy (IPES) or near-edge X-ray absorption fine structure (NEXAFS) for unoccupied states. To be able to compare experimental measurements to theoretical calculations of the electronic structure of alkyl monolayers, such as the recent ones on Si–C bound alkyl chains,⁹ we need to be able to clearly distinguish between intrinsic electronic properties of these monolayers and extrinsic features introduced by experimental techniques. As an example, Figure 1a compares an experimental UPS spectrum of Si/C₁₂H₂₅ taken at low temperature with a total time of exposure to UV radiation of ~20 min, with a theoretically simulated spectrum for C₁₂H₂₅ alkyl chains chemisorbed on Si(111).⁹ The most troubling discrepancy between theory and experiment is the one close in energy to the frontier orbitals involved in charge carrier transport across the junction, that is, the experimental feature located at ~ –3 to –4 eV binding energy (BE) and denoted D. The theoretical spectra, in particular for short chains ($n \leq 12$), show

* Corresponding author: e-mail kahn@princeton.edu; tel +1-609-258-4642; fax +1-609-258-6279.

[†] Princeton University.

[‡] Present address: Air Products and Chemicals, Allentown, PA.

[§] Chiba University.

^{||} Weizmann Institute of Science.

[⊥] University of Würzburg.

[⊗] University of New South Wales.

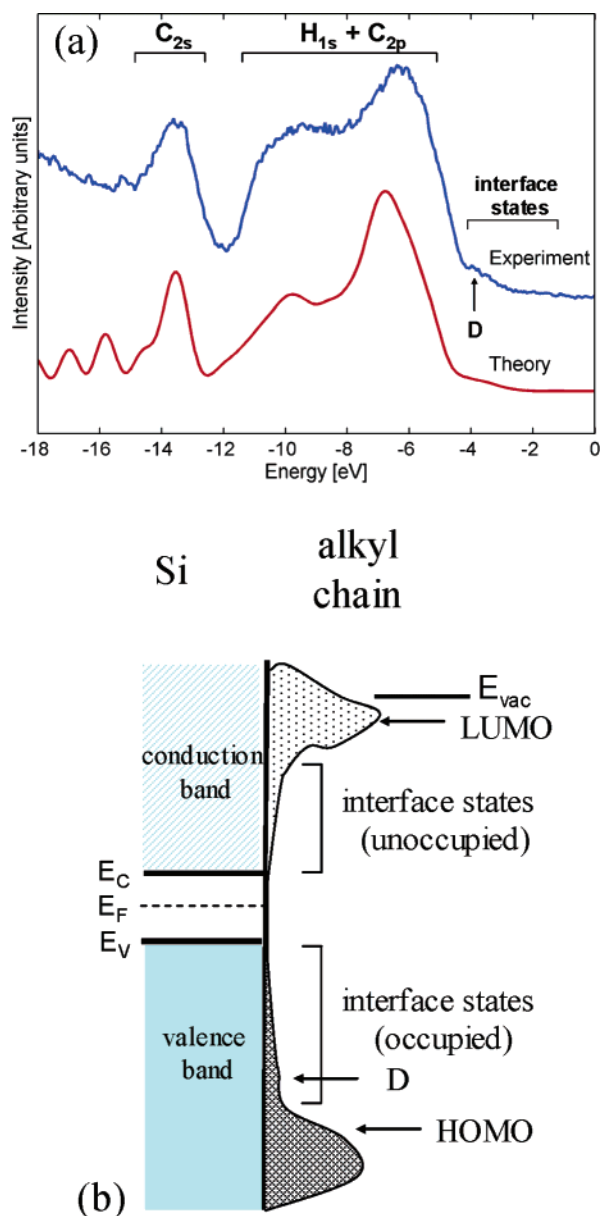


Figure 1. (a) Comparison between the He II spectrum of Si/C₁₂H₂₅, taken at 80 K with 150 meV resolution for a total time of exposure to the UV light of 20 min, and a theoretically simulated UPS spectrum for a C₁₂H₂₅ alkyl chain adsorbed on Si(111).⁹ The energy range of induced interface states that overlaps the molecular energy gap is indicated. D points out the most prominent damage-related feature. The spectrum is dominated by contributions from C–C and C–H bonding on the alkyl chain.^{9,13} (b) Schematic energy diagram of the Si/alkyl chain system, showing the Si electronic structure, the occupied and unoccupied interface states extending in the molecular gap, the approximate positions of the highest occupied and lowest unoccupied molecular orbitals (HOMO and LUMO) of the molecule (away from the interface), and D, the damage-related feature. The occupied state part of panel b relates directly to panel a.

some intensity in that energy range, but the experimental feature appears as a relatively sharp “bump” on the measured spectrum, which varies significantly in intensity with experimental conditions (*vide infra*). We identify this feature as due, in part, to the degradation of the chain under UV irradiation, and we investigate how far its formation obfuscates the interpretation of the results of photoelectron spectroscopies, routinely used to determine the energetics of these systems.

The present paper shows that exposure to UV radiation (He I and He II lines at 21.22 and 40.81 eV, respectively) or soft

X-ray radiation (synchrotron light at around 300 eV), as well as to electron beams, creates essentially the same type of damage to alkyl chain monolayers on Si, GaAs, or SiO₂. Both UPS and NEXAFS point toward the formation of carbon–carbon double bonds (C=C). These results are compared to earlier literature data on damage to bulk and thin film (multi- and monolayer) alkane samples and alkyl-containing polymers. We show that extrapolation of the damage-induced changes in the UPS (and IPES) spectra of the molecular monolayer to short exposure times allows a meaningful extraction of the electronic structure of the pristine monolayer.

Experimental Section

Samples were prepared at the Weizmann Institute of Science and at the University of New South Wales. The preparation of the Si/C_nH_{2n+1},^{10,11} Si/SiO_x/C₁₈H₃₇,¹² and GaAs–S–C_nH_{2n+1}¹³ samples has been described in detail elsewhere. The GaAs–P–O–C_nH_{2n+1} samples were prepared with a version of the method of Hoque *et al.*¹⁴ While the bond is probably through the gallium oxide, from work on other phosphonate oxide¹⁵ interactions we cannot exclude that more than one oxygen of the phosphonate is bound to the surface.¹⁶ The samples were transported to Princeton, Chiba, and Würzburg Universities under N₂ atmosphere. This technique has been shown to produce largely contamination-free monolayers and interfaces.^{10,11,13,17}

The UPS measurements at Princeton University were done with the He I and He II lines of a discharge lamp in ultrahigh vacuum with a total resolution of 150 meV. IPES was performed in the isochromatic mode using a photon detector centered at a fixed energy of 9.2 eV, with a total resolution of 450 meV. To decrease thermal broadening and minimize damage during spectroscopy, the samples were kept at 80 K and the photoemission (inverse photoemission) current was kept at a minimum. The photocurrent density was 2–3 nA/mm² in He I and He II, and the sample current density was ~25 nA/mm² in IPES. Incidence and detection angles are indicated on the figures. The UPS and IPES energy scales were aligned by measuring the position of the Fermi level on a freshly evaporated Au film. The position of the vacuum level, *E*_{vac}, was measured for each surface with the onset of photoemission.

Experiments at Chiba University were performed with a newly constructed high-resolution UPS system consisting of a 200-mm radius energy analyzer (A-1, MBS-Toyama), a microwave discharge He lamp (L-1, MBS), and a toroidal monochromator (M-1, MBS-Toyama). He Iα (21.22 eV) and He II (40.81 eV) radiations were used in the UPS experiments. The monochromatized output of the discharge lamp reduces the background due to photoelectrons excited by higher-energy emission lines, allowing measurement of very low density-of-states in the gap region of the material. The photocurrent density was 1.3 nA/mm² in He I and 0.05 nA/mm² in He II, and the total energy resolution of the measurement was ~25 meV. Spectra were taken at room temperature (RT), 160–170 K, and 35 K.

The NEXAFS data were recorded at the U52-PGM beamline at BESSY in Berlin in the partial electron yield (PEY) mode with a retarding voltage of 100 eV at grazing (70°) incidence of the photon beam and linear s- and p-polarization of the electric field vector. Energy calibration and intensity normalization were performed according to Schöll *et al.*¹⁸ Samples were kept at room temperature, and the beam-line optics was set to illuminate a relatively large spot in order to slow the time scale of damage formation.

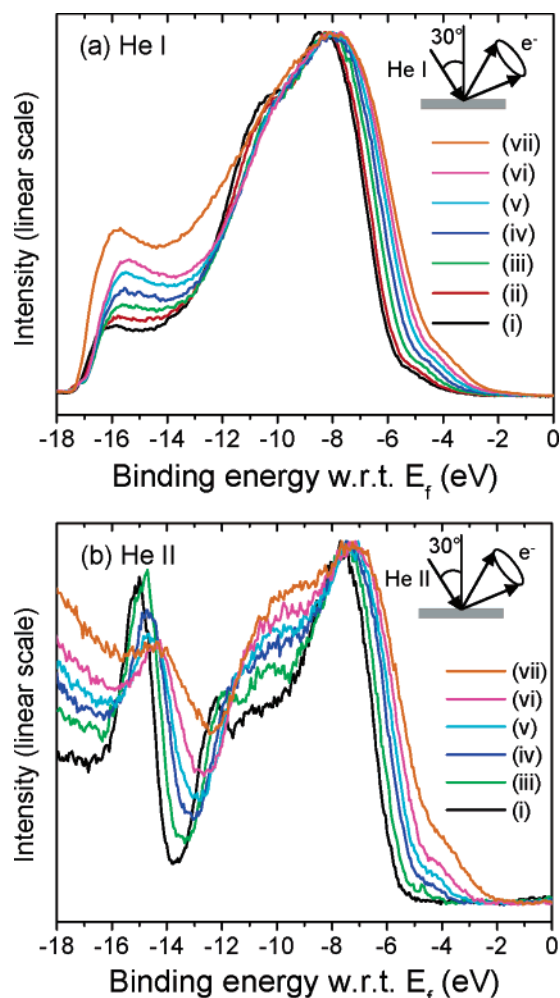


Figure 2. Valence states recorded with (a) the He I line (21.22 eV) and (b) the He II line (40.81 eV) for Si/SiO₂/C₁₈H₃₇ for increasing UV irradiation time. $T_{\text{substrate}} = 80$ K, and the UV lamp optimized for He II radiation (photocurrent density = 2–3 nA/mm²). Total exposure times are (i) 1 min (pristine), (ii) 2 min, (iii) 6 min, (iv) 13 min, (v) 24 min, and (vi) 37 min. The top spectra (vii) correspond to damages induced with higher photon flux for 10 min after step vi: He I setting (photocurrent density = 10–12 nA/mm²).

Results

The effect of the damage, created by UV light on the UPS spectrum of *n*-Si/SiO₂/C₁₈H₃₇ cooled to 80 K is shown in Figure 2. Though He I and He II spectra are presented, the settings for the UV lamp are the same in both types of spectra, that is, optimized for the He II line to minimize the photon flux (photocurrent density ~ 2 –3 nA/mm²). With increasing UV radiation dose, the photoemission spectral features broaden dramatically. In Figure 2a, which also displays the onset of photoemission indicative of the position of the vacuum level of the sample, the broadening affects mostly the low BE side of the spectra. Except for the last spectrum, which corresponds to a much higher photon flux (photocurrent density = 10–12 nA/mm²), UV irradiation produces only a ~ 0.2 eV upward shift of the vacuum level, whereas the top of the density of states (DOS) moves by about 1.3 eV toward the Fermi level. This indicates a change in the ionization energy (IE) of the C₁₈H₃₇ monolayer of more than 1 eV. Note that if this were due to surface charging, the shift would be observed in the opposite direction, that is, toward higher BE.

Further insight is given by Figure 2b, which displays the He II spectra for the same sequence of UV radiation exposures.

With increasing irradiation time, the C2s and C2p carbon peaks at about -15 and -7.5 eV BE,¹⁹ respectively, broaden while shifting toward the Fermi level. At the same time, an additional feature develops at the top of the DOS at about -4 eV BE. These are clear indications that the alkyl chains undergo significant modification during UV irradiation. When the samples are exposed to UV at room temperature instead of 80 K, the degradation is similar but occurs about 10 times faster (not shown here). The degradation is not reversible, even at room temperature.²⁰ Damaged samples warmed to room temperature for up to 24 h still display the same evidence of degradation. That observation rules out the possibility that defects are simply “gauche” defects, which could be annealed out at room temperature. This building up of high-intensity states above the original onset of high intensity of the pristine molecular film has already been reported for polyethylene⁵ and poly(vinylidene fluoride)⁷ and interpreted as corresponding to the formation of C=C double bond.^{5,7}

The 0.7 eV shift of the spectral features toward the Fermi level, measured on the C2s peak (between -15 and -14 eV in Figure 2b), suggests that the film is being doped with acceptor species. A similar effect was reported for 250 Å thick poly-(tetrafluoroethylene) (PTFE) films and attributed to presence of radicals, C=C double bonds, and cross-linked molecules.⁸ However, the shift observed for the alkyl monolayer, which is only ~ 20 Å thick, is somewhat surprising, as no significant “band bending” is expected in the monolayer. It suggests that the charge resulting from the doping either affects the field and the band bending in the Si substrate or is strong enough to affect the energy position of the molecular layer with respect to the substrate energy levels. Note that, in systems such as dye-sensitized solar cells, no band bending occurs but the formation of acceptor levels via chemical doping shifts levels toward lower binding energy, as is seen here.

A closer look at Figure 2a shows that the intensity above the large alkyl-related peak is not related solely to UV-induced damage. The tail of states around -5 eV BE is present even for the “pristine” monolayer, that is, the first spectrum with minimal exposure time, although these states appear not to be visible in the corresponding He II spectrum (Figure 2b). This difference is due to different probing depths in the He I and He II photoemission experiments, compared to the length of the molecule. Indeed, in the case of alkyl chains on Si, the intensity of the tail clearly decreases with increasing chain length (Figure 3a), and the tail is more pronounced for the C₁₈H₃₇ chain directly bound to Si than indirectly bound to GaAs through a phosphonate termination or to Si in the SiO₂ layer (Figure 3b). Results obtained for GaAs–S–C_{*n*}H_{2*n*+1} (not shown here) are similar to those of the phosphonate samples. Accordingly, and in agreement with the recent calculations of Segev et al.⁹ for Si/C₁₂H₂₅, the tail, which is also seen in the theoretical spectrum in Figure 1, is attributed in part to the substrate (Si) density of states and to the associated interface states that penetrate onto the molecules.^{9,13} A schematic representation of these states and of the interface electronic structure is given in Figure 1b. These states are analogous to the metallic density of states that tails into the inorganic^{21–23} or organic^{24,25} semiconductor gap at metal–semiconductor heterointerfaces. These states are readily visible in the He I spectra and less so in the He II spectra, since electrons with an initial binding energy of 5 eV below the Fermi energy have kinetic energies of ~ 11 and ~ 30 eV when photoexcited with He I and He II photons, respectively, and thus have a longer mean free path in the former case.²⁶ In

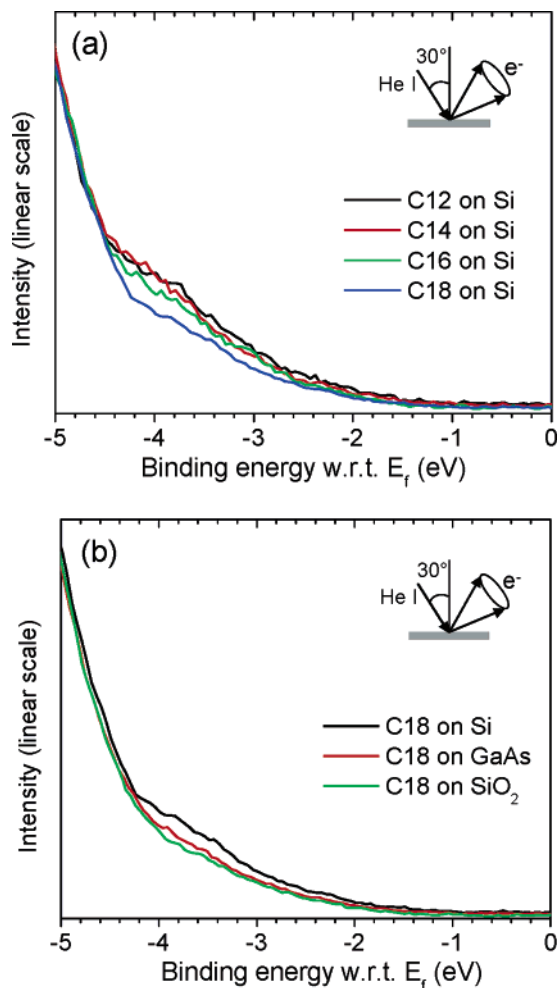


Figure 3. Top of the valence states recorded with He I (21.22 eV) (a) for pristine Si(111)/ C_nH_{2n+1} monolayers with increasing chain length, and (b) for Si/ $C_{18}H_{37}$, Si/SiO_x/ $C_{18}H_{37}$, and GaAs–P–O– $C_{18}H_{37}$. $T_{\text{substrate}} = 80$ K and the UV lamp optimized for He II radiation (photocurrent density = 2–3 nA/mm²). For the sake of clarity, spectra are aligned to offset differences due to different substrates and band bending.

addition, the photoionization cross sections may be different for both energies.

The relative importance of the damage-induced features versus the intrinsic tail of states in the gap region is further examined through the logarithmic plots of the He I intensity recorded from a monolayer of $C_{16}H_{33}$ alkyl chains on Si, held at 35 K for increasing exposure times (Figure 4a). The experimental resolution for this series of experiments is 25 meV. The key result is that the spectrum corresponding to the shortest exposure time (first spectrum with total exposure time of ~96 s), which best represents in this series the electronic structure of the pristine, undamaged SAM, includes significant intensity in the 0–4 eV BE region. The evolution of the intensity integrated in the 0.8–1.4 eV and 2.8–3.4 eV BE window regions, shown in Figure 4b as a function of time of UV-radiation exposure, is an indication of the rate of damage formation. Conversely, the extrapolation of this “additional” intensity down to zero exposure time (Figure 4b) shows that not all the intensity observed between 0 and 4 eV below E_F is induced by defect, and that part is intrinsic to the system. As explained above, the intrinsic part represents the electronic structure of the SAM/substrate interface, which is in part derived from the substrate valence band. In the present case, the relatively sharp drop in intensity close to the Fermi level corresponds to states associated with the Si valence band edge.

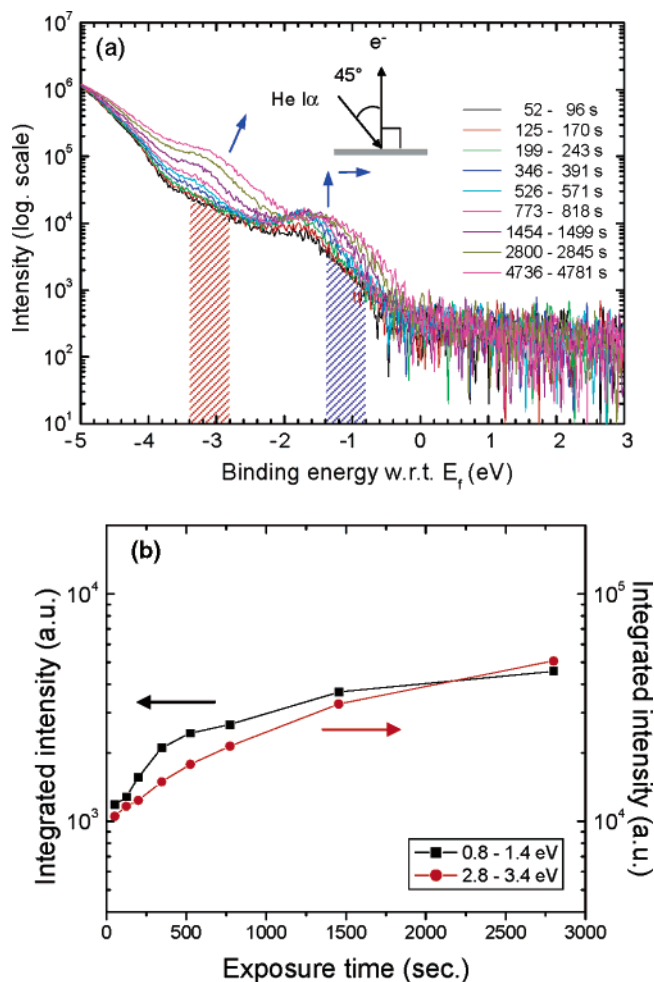


Figure 4. (a) He I spectra of the top of the Si/ $C_{16}H_{33}$ valence states plotted on a logarithmic scale as a function of time of exposure to UV radiation from the UV lamp. The total starting and ending exposure times are indicated for each scan. $T_{\text{substrate}} = 35$ K and the resolution is 25 meV. Arrows outline the evolution of intensity features with exposure to UV radiation. The two shaded areas denote energy windows for intensity integration. (b) Plots of the intensity integrated over energy windows defined in panel a as a function of exposure time.

Another key observation enabled by experiments performed with different resolutions concerns the structural order and inhomogeneities in the SAM system. A comparison of the He II spectra of Si/ $C_{16}H_{33}$ recorded with 150 meV (Princeton University) versus 25 meV (Chiba University) resolution at room temperature (RT) versus low temperature (LT) is given in Figure 5, panels a and b, respectively. The spectra are normalized for the largest peak and arbitrarily shifted in energy to facilitate comparison. As thermal broadening is reduced at low temperature, the spectral features become sharper. However, the similarity between the two RT and LT spectra show that the experimental resolution is not the limiting factor in the line shape of these spectra. Even though the quality of the alkyl/Si SAM is excellent, as is shown elsewhere,^{10,11,17} it appears that inhomogeneities, presumably related to different domain orientations and/or to surface roughness, could contribute to the intrinsic width of the spectra. At the same time, residual differences between the spectra are also attributed to the different data collection geometries afforded by the two UPS systems, implying that some angular dependence due to lateral order in the alkyl monolayer could survive in the photoemission spectra. Indeed, angular dependence has been observed in the past for bulk alkyl systems.^{27–29} In the present case, angular dependence

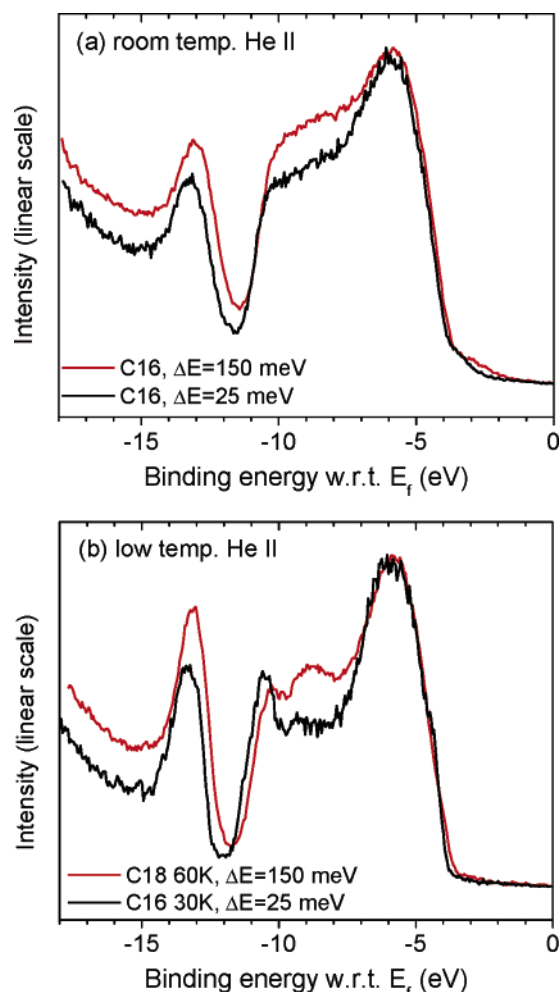


Figure 5. He II spectra of pristine Si/C₁₆H₃₃ recorded with total resolution of 150 and 25 meV at (a) room temperature and (b) low temperature.

would certainly be consistent with recent low-energy electron diffraction data, which show some lateral order in Si(111)/C₁₄H₂₉,¹⁷ and such experiments are underway.

We now turn to the damage induced on these alkyl monolayers by exposure to an electron beam. The He II spectra of Si/C₁₈H₃₇ taken on a pristine layer, and of a similar layer subjected to a 2 min irradiation with 5–15 or 100 eV electrons, are shown in Figure 6. When irradiated with 100 eV electrons (50 nA sample current; current density = 5 μ A/cm²), the alkyl monolayer sustains considerable damage, which, from the line shape of the UPS spectrum, appears to be similar to that observed after a long UV irradiation (see Figure 2b). Assuming that the nature of the damage is similar to that created via UV radiation, this indicates that relatively energetic electrons are efficient in creating C=C double bonds. However, when irradiated with 5–15 eV electrons (800 nA sample current; current density = 40 μ A/cm²) during the IPES experiment, the monolayer exhibits hardly any damage, at least as far as the UPS spectrum is concerned. No significant time evolution of the IPES signal can be detected. This is apparently at odds with the results of Villar et al.,² who reported damage to thin polycrystalline films of hexatriacontane, as seen via high-resolution electron energy loss spectroscopy, when the films were irradiated with electrons with energy higher than 3.5 eV. Although formation of C=C double bonds was suspected, no UPS data were available from these films, and the similarity to the type of damage created here cannot be ascertained.

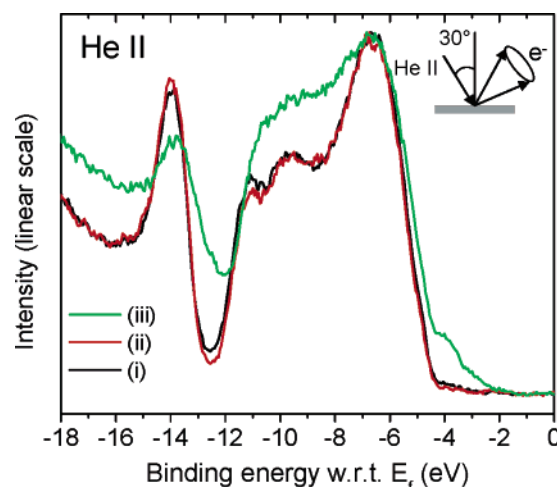


Figure 6. He II spectra of Si/C₁₈H₃₇ recorded (i) before and (ii, iii) after electron beam radiation. $T_{\text{substrate}}$ during measurement and irradiation is 80 K. Irradiation was performed for 2 min (ii) with electron energy scanning between 5 and 15 eV and 200 nA/mm² sample current density, or (iii) with fixed 100 eV energy electrons with sample current density = 50 nA/mm².

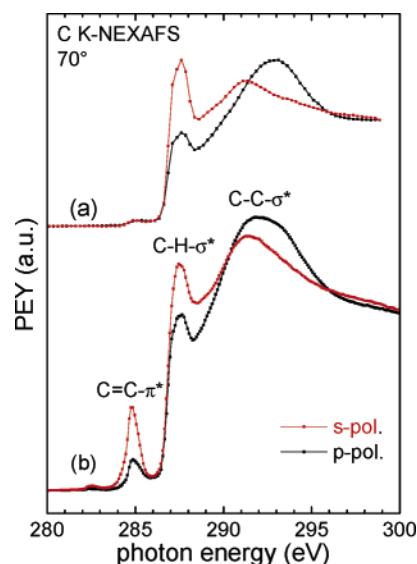


Figure 7. Grazing (70°) incidence NEXAFS spectra of a Si/C₁₈H₃₇ sample, recorded with p- and s-polarization of the incident light and detection in the partial electron yield mode. Each scan (a) was recorded at a fresh spot with an acquisition time of 3 min; for scans (b) the sample was moved to a fresh spot and both scans were recorded at the same spot (p-polarization first) with an acquisition time of 30 min.

The UPS spectra presented above indicate that exposure to both UV radiation and electron beam results in the formation of C=C double bonds in the alkyl chains. Since this type of damage is induced by energetic electrons, it is also likely induced by photons with higher energy than those of the discharge lamp, such as the soft X-ray photons used for core-level ionization in NEXAFS. Of course, radiation damage in this case may arise from the Auger decay after core ionization, creating a repulsive double-hole final state, or from the abundant secondary electrons, or from both. Undamaged alkyl chains have only carbon–carbon σ bonds and, therefore, the presence of a π^* level associated with a C=C double bond should have a signature in NEXAFS. This point is clearly demonstrated in Figure 7, which shows a distinct π^* resonance at about 285 eV emerging with increasing irradiation that is not characteristic of a pristine alkyl chain.^{30–34} Each of the two spectra denoted

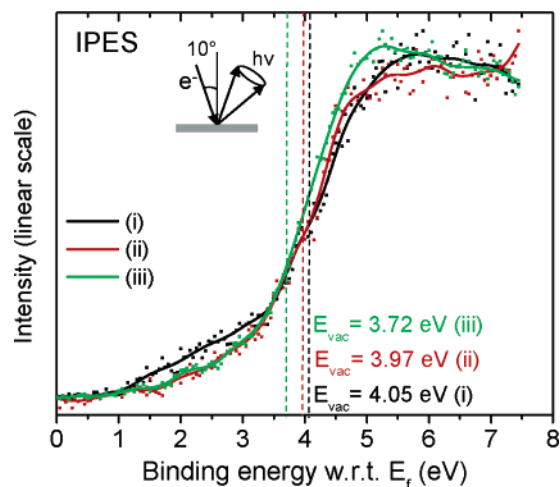


Figure 8. IPES spectra of Si/C₁₈H₃₇ recorded (i) before and (ii) after 100 eV electron beam irradiation; and (iii) of a pristine GaAs-S-C₁₈H₃₇. $T_{\text{substrate}} = 80$ K in all cases. Dashed lines indicate the position of the vacuum level deduced from the onset of photoemission for each sample.

(a) was recorded at a fresh spot on the Si/C₁₈H₃₇ sample (the vertical spot size of the synchrotron beam was smaller than 500 μm), with an acquisition time of 3 min. The two spectra denoted (b) were recorded at the same, initially fresh, spot (p-polarization first) with a total acquisition time of 30 min. The dichroic behavior of the π^* peak, which is much stronger for s-polarization, may indicate a preferential generation of π -bonds along the alkyl chains, in contrast to cross-linking. The latter would lead to π -orbitals parallel to the substrate and hence stronger absorption in p-polarization. In addition to the appearance of π^* intensity, the NEXAFS spectra show a substantial change in the intensity of the C–H σ^* resonance relative to the C–C σ^* . In the pristine film (spectrum (a)) the intensity ratio (C–H $\sigma^*/\text{C–C } \sigma^*$) is 0.56 for p- and 1.14 for s-polarization, whereas the values change to 0.65 for p- and 0.92 for s-polarization upon damage. This can be explained by a change in chain orientation due to C=C double-bond formation with different bonding angles within the chains. We note that extensive NEXAFS studies on radiation-induced changes of SAMs have been published previously.^{35–38}

The signature of the *occupied* state corresponding to the C=C double bond (π) is clearly visible in the UPS spectra of the damaged alkyl monolayers (Figures 2–4). Therefore, we can expect to see the corresponding π^* unoccupied state also in the IPES spectra. IPES spectra recorded for pristine C₁₈H₃₇ monolayer on Si and GaAs are displayed in Figure 8 and compared to the spectrum of a C₁₈H₃₇ monolayer on Si damaged with 100 eV electrons. The position of the vacuum level is indicated in each case. Surprisingly, no significant difference is observed between the pristine and damaged films. Although the lack of sensitivity to the 100 eV electron-induced damage is presently not understood, we can rule out that the two pristine layers were in fact rapidly damaged by the electron beam at the start of the IPES experiment, since no damage was observed with UPS following the IPES experiment.

Undamaged alkyl chains have been reported to display very small, and even negative, electron affinity.^{39,40} Assuming a similar electronic structure of the present films, the substantial intensity tail between 1 and 3 eV above the Fermi level (or 1–3 eV below the vacuum level) in the IPES spectra of the pristine C₁₈H₃₇ monolayer cannot be attributed to the LUMO of the molecular film per se. Recent computations of the electronic structure of the Si/C₁₀H₂₁ and Si/C₁₂H₂₅ systems,⁹ aided by UPS and IPES experimental data, evaluate the

magnitude of the energy gap between HOMO and LUMO of the molecular film itself at about 9 eV, thus placing the LUMO above the observed intensity tail. Since the IPES experiment is performed with 5–15 eV electrons, which have a relatively long mean free path, the entire molecular film as well as the interface is probed. Thus the IPES intensity tail, much like the UPS intrinsic intensity tail, is attributed to the contribution from the molecule/substrate interface and from the interface states that tail into the molecular chain (Figure 1b), in agreement with the theoretical modeling of the Si/C_{*n*}H_{2*n*+1} systems.⁹

Summary

The effect of UV radiation (21.2 and 40.8 eV), soft X-ray irradiation (300 eV), and electron beam-induced damage on alkyl monolayers (C_{*n*}H_{2*n*+1}, *n* = 12–18) on Si, SiO₂, and GaAs were investigated via UPS, IPES, and NEXAFS. Damage consisting of C=C double-bond formation occurs with all types of sources. Though He I and He II radiation damage can be minimized by reducing the exposure time (less than 1 min with 10 nA photocurrent) and by cooling the sample to low temperature, the results indicate a significant impact of damage on the electron spectroscopy data, which must be taken into account in order to correctly interpret the electronic structure of these systems. Extrapolation of the effect of damage to short exposure time allows the determination of the electronic structure of the pristine monolayer. Finally, the similarity between the damage induced on alkyl monolayers chemisorbed on three different substrates via three different chemistries strongly suggests that the process is a very general one and should occur on, among other systems, the widely used SAM system of alkanethiols on Au.

Acknowledgment. Work at Princeton University was supported by the National Science Foundation (DMR-0408589) and the Princeton MRSEC of the National Science Foundation (DMR-0213706). Work at Chiba University was partly supported by the 21st Century Center-of-Excellence program of MEXT (Frontiers of Super-Functionality Organic Devices, Chiba University) and a Grant-in-Aid for Creative Scientific Research of JSPS (14GS0213). The Weizmann Institute of Science efforts were supported in part by the Bikura fund of the Israel Science Foundation, the Kimmel Center for Nanoscale Science and the Gerhard Schmidt Minerva Center for Supramolecular Architecture. The NEXAFS work was financially supported by the BMBF (Projects 05 SF8 WWA 7 and 05 KS1 WWA 5). E.U. thanks the Fonds der Chemischen Industrie for financial support.

References and Notes

- (1) Ueno, N.; Sugita, K.; Koga, O.; Suzuki, S. *Jpn. J. Appl. Phys.* **1983**, 22, 1613.
- (2) Villar, M. R.; Schott, M.; Pfluger, P. *J. Chem. Phys.* **1990**, 92, 5722.
- (3) Buncik, M. C.; Thomas, D. E.; McKinny, K. S.; Jahan, M. S. *Appl. Surf. Sci.* **2000**, 156, 97.
- (4) Heister, K.; Zharnikov, M.; Grunze, M.; Johansson, L. S. O.; Ulman, A. *Langmuir* **2001**, 17, 8.
- (5) Ono, M.; Morikawa, E. *J. Phys. Chem. B* **2004**, 108, 1894.
- (6) Wagner, A. J.; Han, K.; Vaught, A. L.; Fairbrother, D. H. *J. Phys. Chem. B* **2000**, 104, 3291.
- (7) Morikawa, E.; Choi, J.; Manohara, H. M.; Ishii, H.; Seki, K.; Okudaira, K. K.; Ueno, N. *J. Appl. Phys.* **2000**, 87, 4010.
- (8) Ono, M.; Yamane, H.; Fukagawa, H.; Kera, S.; Yoshimura, D.; Morikawa, E.; Seki, K.; Ueno, N. *IPAP Conf. Series* **2005**, 6, 27.
- (9) (a) Segev, L.; Salomon, A.; Natan, A.; Cahen, D.; Kronik, L.; Amy, F.; Chan, C. K.; Kahn, A. *Phys. Rev. B* **2006** (in press). (b) Salomon, A.; Böcking, T.; Seitz, O.; Amy, F.; Chan, C.; Kahn, A.; and Cahen, D. (submitted for publication).

- (10) Salomon, A.; Boecking, T.; Chan, C. K.; Amy, F.; Girshevitz, O.; Cahen, D.; Kahn, A. *Phys. Rev. Lett.* **2005**, *95*, 266807.
- (11) Seitz, O.; Boecking, T.; Salomon, A.; Gooding, J. J.; Cahen, D. *Langmuir* **2006**, *22*, 6915.
- (12) Styrkas, D. A.; Keddie, L. J.; Lu, J. R.; Su, T. J.; Zhdan, P. A. *J. Appl. Phys.* **1999**, *85*, 868.
- (13) Nesher, G.; Vilan, A.; Cohen, H.; Cahen, D.; Amy, F.; Chan, C. K.; Hwang, J.; Kahn, A. *J. Phys. Chem.* **2006**, *110*, 14363.
- (14) Hoque, E.; DeRose, J. A.; Kulik, G.; Hoffmann, P.; Mathieu, H. J.; Bhushan, B. *J. Phys. Chem. B* **2006**, *110*, 10855.
- (15) Rego, A. M. B. d.; Ferraria, A. M.; Beghdadi, J. E.; Debontridder, F.; Brogueira, P.; Naaman, R.; Vilar, M. R. *Langmuir* **2005**, *21*, 8765.
- (16) Kanan, S. M.; Tripp, C. P. *Langmuir* **2001**, *17*, 2213.
- (17) Kahn, A.; Zhao, W.; Ha, S.; Chan, C.; Amy, F.; Boecking, T.; Cahen, D.; Salomon, A.; Seitz, O. Manuscript in preparation. 2006.
- (18) Schöll, A.; Zou, Y.; Schmidt, T.; Fink, R.; Umbach, E. *J. Electron. Spectrosc. Relat. Phenom.* **2003**, *129*, 1.
- (19) Duwez, A. S.; Paolo, S. D.; Ghijsen, J.; Riga, J.; Deleuze, M.; Delhalle, J. *J. Phys. Chem. B* **1997**, *101*, 884.
- (20) Cohen, S. R.; Naaman, R.; Sagiv, J. *J. Phys. Chem.* **1986**, *90*, 3054.
- (21) Heine, V. *Phys. Rev.* **1965**, *138*, A1689.
- (22) Tejedor, C.; Flores, F.; Louis, E. *J. Phys. C: Solid State* **1977**, *10*, 2163.
- (23) Louie, S. G.; Cohen, M. L. *Phys. Rev. B* **1976**, *13*, 2461.
- (24) Vazquez, H.; Oszwaldowski, R.; Pou, P.; Ortega, J. P., R.; Flores, F.; Kahn, A. *Europhys. Lett.* **2004**, *65*, 802.
- (25) Sun, Q.; Selloni, A.; Scoles, G. *ChemPhysChem* **2005**, *6*, 1906.
- (26) Zangwill, A. *Physics at surfaces*; Cambridge University Press: Cambridge, U.K., 1988.
- (27) Seki, K.; Ueno, N.; Karlsson, U. O.; Engelhardt, R.; Koch, E. E. *Chem. Phys.* **1986**, *105*, 247.
- (28) Ueno, N.; Gaedeke, W.; Koch, E. E.; Engelhardt, R.; Dudde, R.; Laxhuber, L.; Moewald, H. *J. Mol. Electron.* **1985**, *1*, 19.
- (29) Ueno, N.; Seki, K.; Sato, N.; Fujimoto, H.; Kuramochi, T.; Sugita, K.; Inokuchi, H. *Phys. Rev. B* **1990**, *41*, 1176.
- (30) Stöhr, J.; Outka, D. A.; Baberschke, K.; Arvanitis, D.; Horsley, J. A. *Phys. Rev. B* **1987**, *36*, 2976.
- (31) Bagus, P. S.; Weiss, K.; Schertel, A.; Woll, C.; Braun, W.; Hellwig, C.; Jung, C. *Chem. Phys. Lett.* **1996**, *248*, 129.
- (32) Vaterlein, P.; Fink, R.; Umbach, E.; Wurth, W. *J. Chem. Phys.* **1998**, *108*, 3313.
- (33) Weiss, K.; Bagus, P. S.; Wöll, C. *J. Chem. Phys.* **1999**, *111*, 6834.
- (34) Schöll, A.; Fink, R.; Umbach, E.; Mitchell, G. E.; Urquhart, S. G.; Ade, H. *Chem. Phys. Lett.* **2003**, *370*, 834.
- (35) Zharnikov, M.; Frey, S.; Götzhäuser, A.; Geyer, W.; Grunze, M. *Phys. Chem. Chem. Phys.* **1999**, *1*, 3163.
- (36) Heister, K.; Frey, S.; Gölzhauser, A.; Ulman, A.; Zharnikov, M. *J. Phys. Chem. B* **1999**, *103*, 11098.
- (37) Feulner, P.; Niedermayer, T.; Eberle, K.; Schneider, R.; Menzel, D.; Lehner, A.; Schmich, E.; Shaporenko, A.; Tai, Y.; Zharnikov, M. *Phys. Rev. Lett.* **2004**, *93*, 178302.
- (38) Frey, S.; Rong, H.-T.; Heister, K.; Yang, Y.-J.; Buck, M.; Zharnikov, M. *Langmuir* **2002**, *18*, 3142.
- (39) Ueno, N.; Sugita, K.; Seki, K.; Inokuchi, H. *Phys. Rev. B* **1986**, *34*, 6386.
- (40) Vilar, M. R.; Blatter, G.; Pfluger, P.; Heyman, M.; Schott, M. *EuroPhys. Lett.* **1988**, *5*, 375.